PACS numbers: 42.55.Rz; 42.60.Jf
DOI: 10.1070/QE2008v038n09ABEH013640

Spectra, temporal structure, and angular directivity of laser radiation of a Yb : YAG crystal and ytterbium glass pumped by low-coherence radiation from a F_2^+ : LiF colour centre laser

N.E. Bykovsky, Yu.V. Senatsky

Abstract. **By focusing radiation from a F_2^+ : LiF colour centre laser (emitting in the range from 0.89 to 0.95 μm) on plates of a Yb : YAG crystal with the 20 % concentration of Yb and of ytterbium glass with the 10 % concentration of Yb, we observed nanosecond radiation pulses of Yb^{3+} ions in the spectral region from 1.00 to 1.06 μm with the spectral width up to 20 nm in Yb : YAG and up to 50 nm in the ytterbium glass. Lasing appeared in the active medium in the region of excitation of the SBS of pump radiation with a diameter less than 200 μm. The angular divergence of the broadband laser radiation ($10^{-3} - 10^{-4}$ rad) was one – two orders of magnitude smaller than the diffraction limit. The mechanism of generation of short broadband high-directional laser pulses in the spatial structure of thin layers with inversion produced in the region of propagation of an intense acoustic wave in the medium is discussed. The interpretation of experimental data on the angular divergence of radiation is based on a new concept of the spatial distribution of the electromagnetic field of a photon not in the form of a travelling wave but with the field structures located in fixed positions along the propagation direction. The features of the temporal picture and narrowband lasing spectra of Yb : YAG and ytterbium glass in a resonator upon relaxation of the SBS excitation region in the active medium are considered. The possibility of diagnostics of medium parameters using the shift of spectra of the lasing at the resonator modes in different sites of the SBS excitation region is discussed.**

Keywords: *Yb : YAG crystal, ytterbium glass, broadband lasing, pump F_2^+ : LiF laser, near-diffraction free propagation.*

1. Introduction

Investigations of ytterbium-doped laser crystals, glasses, and ceramics attract great recent attention [1 – 6]. Works devoted to the development of high-power lasers [7 – 11] stimulated the study of processes of inversion formation and dumping, generation and amplification of radiation in media with high concentrations of Yb^{3+} ions at high pumping intensities [2, 3, 5, 6]. Media doped with Yb^{3+} ions are usually pumped by semiconductor diodes emitting at ~ 0.9 μm. We pumped a Yb : YAG crystal containing 20% of ytterbium by short (20 – 30 ns) pulses from a broadband (0.89 – 0.95 μm) F_2^+ : LiF colour centre laser (CCL) [3]. The intensity of laser radiation focused on samples could exceed 1 GW cm^{-2} [3]. In this case, the interaction of pump radiation with the optical medium was essentially nonlinear, which could lead to stimulated scattering, surface and volume damage and affect the lasing parameters of ytterbium-doped media. The dynamics of lasing in a Yb : YAG crystal at 1.03 and 1.05 μm pumped by a CCL was investigated in [3]. In this paper, we continue the study of lasing in a Yb : YAG crystal and ytterbium-doped phosphate glass pumped by a CCL. We observed stimulated scattering of broadband CCL radiation in the YAG crystal and glass and investigated the features of temporal, spectral, and angular characteristics of radiation of ytterbium in the Yb : YAG crystal and glass. We also observed anomalously broad (up to 50 nm in glass and up to 20 nm in the Yb:YAG crystal) spectra of high-directional radiation of ytterbium pumped by a F_2^+ : LiF CCL. These effects are interpreted and the physical model of processes proceeding in the active medium during its nonlinear interaction with pump radiation is proposed to explain the spectral, temporal and angular characteristics of radiation generated by ytterbium-doped media. The experimental data on the angular divergence of radiation are interpreted by using a new concept of the spatial distribution of the electromagnetic field of a photon not in the form of a travelling wave but with the field structures (maxima, minima, nodes) located in fixed positions along the propagation direction.

N.E. Bykovsky, Yu.V. Senatsky P.N. Lebedev Physics Institute, Russian Academy of Sciences, Leninsky prosp. 53, 119991 Moscow, Russia; e-mail: senatsky@sci.lebedev.ru, nbykovsky@sci.lebedev.ru

Received 23 May 2007; revision received 29 October 2007
Kvantovaya Elektronika **38** (9) 813 – 822 (2008)
Translated by M.N. Sapozhnikov

2. Experiments on pumping ytterbium-doped media by a F_2^+ : LiF CCL

Pumping experiments were performed by using a setup described in detail in [3, 12, 13]. Figure 1 presents the simplified scheme of the setup. Samples [plane – parallel 2-mm-thick Yb : YAG crystal (20 % of Yb) plates or 3-mm-thick ytterbium-doped glass (10 % of Yb) plates] were mounted in a resonator of length $L \approx 20$ mm formed by plane mirrors M8 and M9. Samples were pumped by pulses of focused radiation from a CCL through mirror M8 with the reflectance ~ 100 % at ~ 1 μm transmitting 80 % – 90 % of pump radiation. The pump beam propagated close to the normal to the resonator mirrors. The reflectance of mirror M9 at ~ 1 μm was 30 % (for Yb : YAG) or 70 % (for ytterbium glass). This setup was also used to record

stimulated scattering. These experiments were performed with ytterbium-doped and pure samples [12]. The resonator mirrors in this case were absent and CCL radiation was focused directly on samples. The energy, spectrum, shape and duration of the pump, stimulated scattering and laser pulses of ytterbium were recorded by deflecting parts of radiation to calorimeters, photodetectors, and a spectrograph [3, 12, 13]. The shape and duration of pulses were recorded with a two-channel oscilloscope with a resolution of ~ 4 ns, and the pump and lasing spectra were recorded with a STE-1 spectrograph on an IR film or on the screen of an image converter.

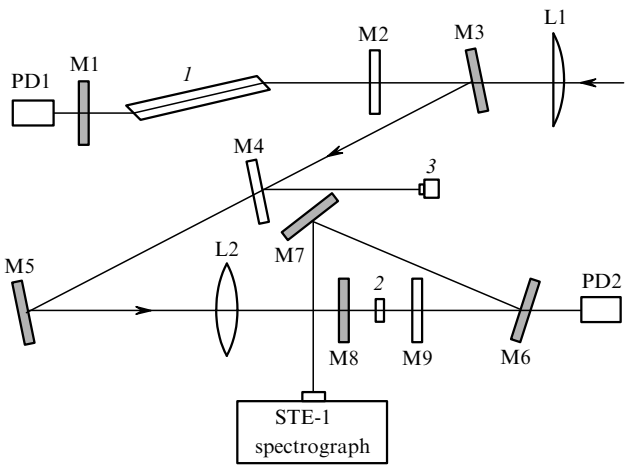

Figure 1. Scheme of the experimental setup: (*1*) active element of a CCL; (*2*) ytterbium-doped plate in the resonator with mirrors M8 and M9; (*3*) calorimeter; (M1, M2) CCL resonator mirrors; (M3 – M7) steering mirrors for CCL and ytterbium laser radiation; (L1, L2) lenses; (PD1, PD2) photodetectors.

Experiments were performed at room temperature in the single-pulse regime. A colour centre laser ($L \simeq 30$ cm) was pumped through lens L1 by pulses from a passively Q-switched ruby laser. At the high amplification level in F_2^+ : LiF, generation in the CCL was developed during a few round trips in the resonator. The CCL pulse shape repeated in fact that of the ruby laser pulse [3]. The CCL pulses had duration of 20 – 30 ns and their spectrum was in the range from 0.89 to 0.95 μm, with the maximum at ~ 0.92 μm [3]. A short lasing development time and a broad width of the spectrum with a smooth envelope suggest that the CCL radiation had a low coherence. The width $\Delta\nu_p$ of the pump spectrum could exceed 30 nm, which corresponds to the radiation coherence length $l_c \leqslant 30$ μm. The CCL energy varied within 50 – 150 mJ. In most experiments, samples in the resonator were exposed to the radiation of energy 60 – 70 mJ. The CCL beam divergence was $(2-3)\times10^{-3}$ rad and the beam diameter was 5 – 6 mm. This radiation focused by lens L2 with the focal distance of 120 mm produced the radiation intensity distribution $I(r)$ (r is the radius of the excited region) in the surface layers of samples with the maximum at the pump beam axis. The minimal size $2r$ of the focal spot on the sample surface was ~ 250 μm. The CCL radiation intensity was varied within 0.5 – 5 GW cm^{-2} by moving the lens. High pump intensities could produce damages in samples. In this case, a new, undamaged site of the sample was irradiated by next pulses.

Lasing in a Yb : YAG crystal was observed at pump intensities exceeding 0.5 GW cm^{-2}. The output energy did not exceed 0.5 mJ. Figures 2 and 3 show lasing oscillograms recorded for one shot and corresponding spectrograms. The first of a series of laser pulses appeared during the pump pulse, while the next pulses were developed after the end of the pump pulse and were delayed by tens and hundreds of nanoseconds (Figs 2 and 3), in accordance with results obtained in [3]. The lasing spectra were recorded within an angle of $\sim 10^{-2}$ rad, which was determined by the spectrograph slit height and a distance (~ 1 m) to the sample. No focusing of radiation on the spectrograph slit was performed. Radiation from the axial lasing region was directed to the lower part of the slit. Figures 2 and 3 demonstrate separate laser lines (line lasing) in the region of transitions in ytterbium at 1.03 and 1.05 μm. The intervals between closely spaced lines correspond to the distance between the longitudinal modes of a Fabry – Perot resonator with a selector, which was a sample itself. According to data obtained in [3], line lasing at low pump intensities appeared first at ~ 1.05 μm. As the pump intensity was increased, line lasing was observed simultaneously at 1.03 and 1.05 μm (Fig. 2), and at the maximum pump intensity, it was observed at 1.03 μm (Fig. 3). Along with narrowband lasing, broadband lasing was also observed virtually in each pulse. Spectral bands of width up to 20 nm were extended to the blue (up to 1.0 μm) and red (up to 1.06 μm) parts of the spectrum far beyond the regions near 1.03 and 1.05 μm in which lasing in a Yb : YAG crystal is usually observed. As the pump intensity was increased, the broadband lasing spectra shifted to the blue (Fig. 3).

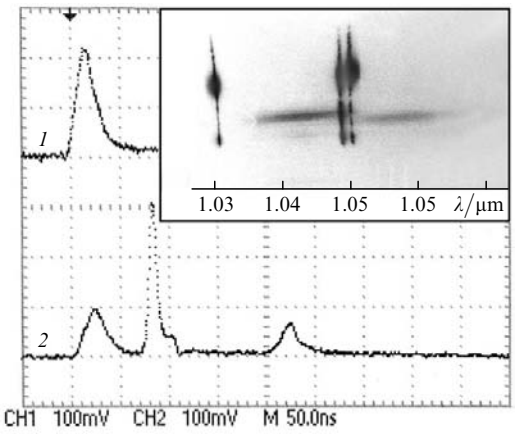

Figure 2. Oscillograms of pump (*1*) and laser (*2*) pulses, and the lasing spectrum of the Yb : YAG crystal in the 1.03 – 1.06-μm region.

Lasing in the ytterbium glass (Figs 4 and 5) appeared at pump intensities ~ 5 GW cm^{-2} and was accompanied, as a rule, by the local damage of samples. The lasing energy did not exceed 0.1 mJ. The oscillograms of lasing in the glass as the lasing in the Yb : YAG crystal exhibit several nanosecond pulses delayed with respect to the pump pulse (Fig. 5). The spectrograms demonstrate narrowband (in the region from 1.02 to 1.05 μm) and broadband (1.00 – 1.06 μm) lasing spectra (Figs 4 and 5). The total width of two spectral bands of the ytterbium glass emission exceeded 50 nm (Fig. 4).

The narrowband and broadband lasing spectra in the glass and Yb : YAG were recorded from the spectrograph

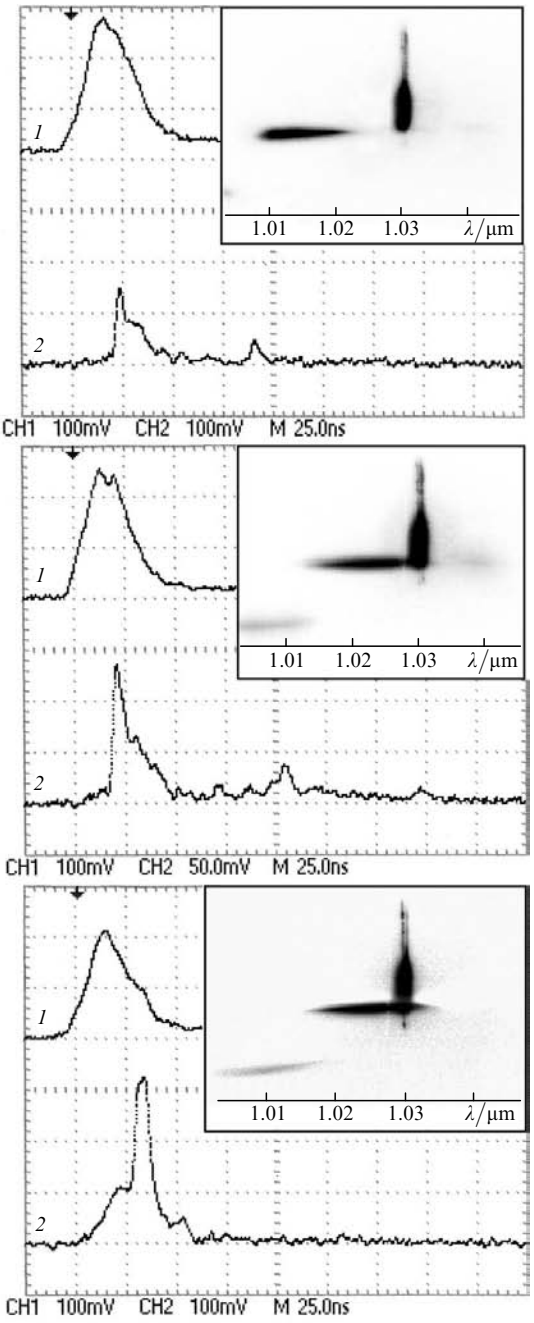

Figure 3. Oscillograms of pump (*1*) and laser pulses in the Yb:YAG crystal (*2*) and lasing spectra in the 1.01 – 1.03-μm region for three CCL pulses with energies 100, 125, and 150 mJ (from bottom to top).

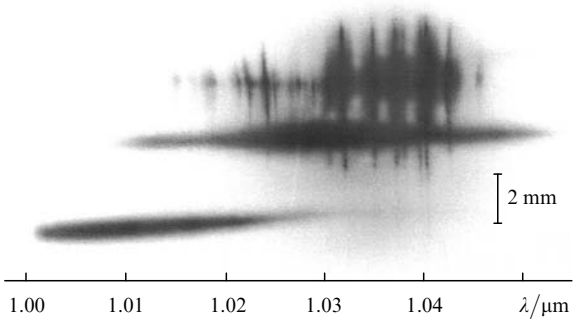

Figure 4. Lasing spectra of the ytterbium glass in the 1.00 – 1.05-μm region.

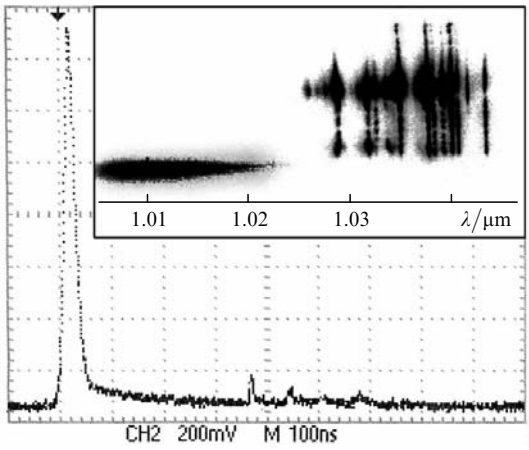

Figure 5. Oscillograms of laser pulses in the ytterbium glass and lasing spectra in the 1.00 – 1.04-μm region.

slit parts located at different heights (Figs 2 – 5). The spectra of ytterbium were recorded when the entrance slit of the spectrograph was in the far-field diffraction zone with respect to the radiation source. The experimental data demonstrate a high directivity of broadband radiation beams. The angular divergence of this radiation, estimated from the size of spots on the slit (see Figs 2 – 5), did not exceed usually 10^{-3} rad and 10^{-4} rad in some pulses. At the same time, the angular divergence due to diffraction for the lasing region with $r \approx 100$ μm is $\sim 10^{-2}$ rad. Thus, the angular directivity of radiation from the lasing region could exceed the diffraction limit by one – two orders of magnitude.

The generation of several pulses in the ytterbium laser delayed with respect to the pump pulse (Figs 2, 3, 5) was explained in [3] by heating (upon pumping) and rapid cooling processes in the quasi-three-level active medium, which changed the population of the working levels of the laser transition. However, the nature of these processes was not investigated in [3].

The analysis of the spectral features, the temporal picture and angular directivity of laser radiation in the ytterbium-doped glass and Yb:YAG crystal taking into account the stimulated scattering of pump radiation in these media, which was started in [13], is continued in this paper.

3. Stimulated Brillouin scattering of pump radiation and inversion distribution in the active medium

At pump intensities from 0.5 to 5 GW cm^{-2} used in our experiments, we observed intense pulses of CCL radiation scattered in crystal and glass samples in a broad angular range in the forward (from 0 to 30°) and backward (from 0 to 50°) directions [12]. Although the spectra of scattered radiation were not studied due to their large width, the temporal and angular characteristics of scattered radiation allow one to interpret the observed scattering as stimulated scattering (SBS and SRS) of broadband CCL radiation in crystals and glasses. For example, we observed radiation pulses reflected back to the CCL aperture (at an angle of 180°) and transmitted through the sample (YAG crystal) (Fig. 6), which is typical for SBS. Backward reflection was

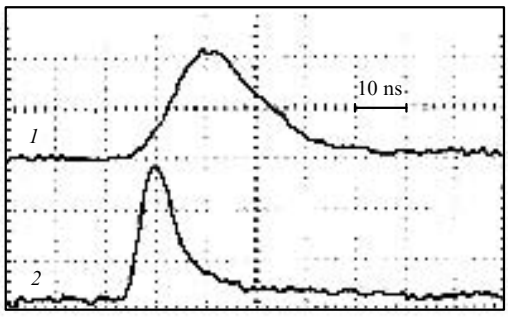

Figure 6. Oscillograms of the radiation pulse reflected back from a YAG crystal plate (at an angle of 180° with respect to the pump beam) (*1*) and of the CCL pulse transmitted through the plate (*2*).

also recorded when a sample was mounted at an angle (from 5° to the Brewster angle) to the CCL beam axis.

By comparing these data with SBS characteristics [14, 15], we conclude that we observed the SBS of broadband CCL radiation in samples. The study of temporal and angular characteristics of radiation scattered at angles from 0 to 50° in the forward and backward directions [12] also suggests that the intense SRS of CCL radiation was observed in crystals and glasses. Note that the pump intensity (0.5 GW cm^{-2}) at which the stimulated scattering of low-coherence radiation was already observed is almost an order of magnitude lower than the coherent pump intensity typical for excitation of SBS and SRS in glasses and crystals (see, for example, [15]).

When samples were exposed to 4 – 5-GW cm^{-2} radiation from the CCL, sites of transverse size 200 – 300 μm with the damaged structure appeared near the sample surface at a depth of 5 – 50 μm (Fig. 7). Such sites were observed in the YAG crystal, glass, and quartz irradiated by CCL pulses [12]. The damage produced by intense low-coherence radiation differs from the damage of optical media caused by highly coherent radiation (see, for example, [16]). This fact is probably explained by different damage mechanisms. Note that studies of the damage of transparent dielectrics by highly coherent laser radiation did not reveal its relation with SBS [15], whereas photographs in Fig. 7 demonstrate the energy release in the surface layer of samples, which can be caused by the SBS of CCL radiation in this layer.

The nonlinear phenomena observed in experiments and the lasing properties of ytterbium-doped media were interpreted by assuming that the SBS of low-coherence CCL radiation is accompanied by the formation of a sequence of longitudinal shock acoustic waves propagating along the pump beam in a thin surface layer of the medium [12]. The formation of shock acoustic waves on an elastic nonlinearity upon SBS was considered in theoretical papers [17, 18]; however, the results obtained in these papers were not confirmed so far in coherent pumping experiments. The appearance of shock waves upon low-coherence pumping and their absence upon coherent pumping can be caused by the difference in the conditions of radiation scattering by short-lived small-scale density fluctuations and stationary inhomogeneities in the medium in these two cases. Upon coherent pumping, SBS by density fluctuations is observed [14, 15]. Stationary inhomogeneities cannot be the sources of acoustic waves upon coherent pumping because constant generation of such waves at the same place near a local inhomogeneity will lead to their mutual quenching due to interference and, therefore, SBS will not appear in this case. In the case of incoherent pumping, stationary inhomogeneities can play the role of seeds for excitation of acoustic waves and stimulated scattering [12]. Indeed, if the duration of a single short pump spike is $t_s < T/2$ (T is the period of a hypersonic wave), the scattering of such a pulse by the inhomogeneity can lead to excitation of an acoustic wave in the medium. The next pump spikes will enhance the acoustic wave. In solids this mechanism can involve different scattering centres such as lattice inhomogeneities, small inclusions, etc. A comparatively large amplitude of scattering by stationary inhomogeneities (compared to scattering by density fluctuations) and the high intensity of individual spikes of the broadband low-coherence pumping (compared to the average pump intensity) should reduce the SBS threshold. The condition $t_s < T/2$ was fulfilled in our experiment because $t_s \sim 1/\Delta\nu_p < 0.1$ ps, and the period of a hypersonic wave excited by optical radiation in crystals and glasses is tens of picoseconds [14, 15].

Consider the features of the inversion distribution in the medium upon SBS of pump radiation. The dynamic grating of acoustic waves produced in samples over the length $l \geqslant l_c$ played the role of an additional external mirror for the CCL and efficiently reflected incident radiation, preventing its propagation inside a crystal or glass. The penetration depth of hypersonic waves into the medium is $l \approx 1/\alpha$ ($\alpha = 10^2 - 10^3$ cm^{-1} is the hypersound attenuation coefficient) [15]. Thus, the excitation region of SBS (and SRS) in the medium is a surface layer of thickness $l < 100$ μm. The heat release caused by the dissipation of energy of acoustic waves and phonons excited in the medium upon SRS of CCL radiation occurred in this layer. Inversion was also mainly produced in this thin layer. The maximum energy density stored in Yb : YAG containing 20 % of Yb ($N_0 = 2.9 \times 10^{21}$ cm^{-3}) upon excitation of all Yb^{3+} ions to the $^2F_{5/2}$ metastable level was estimated as ~ 500 J cm^{-3}. Even for such an extremely large energy in the volume of a Yb : YAG crystal cylinder of diameter 250 μm and length 100 μm, the energy stored in inversion does not exceed, according to estimates, 2.5 mJ, which corresponds to the low lasing energy of ytterbium in experiments. A part of the pump energy was absorbed by ytterbium ions beyond the region of SBS excitation, and the other part escaped from the sample. In this case, the profile of the population on the metastable level of ytterbium was formed, which decreased over the sample length along the pump beam.

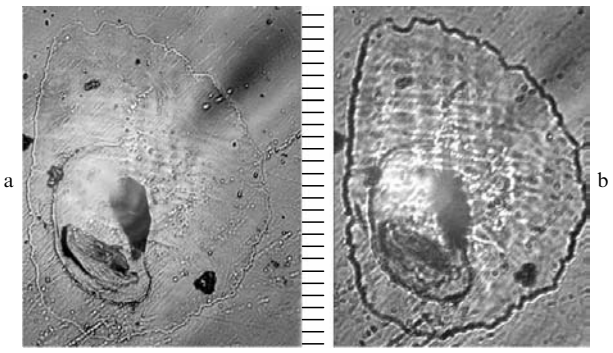

Figure 7. Photographs of the YAG crystal surface (a) and of the region lying at a depth of 7 – 10 μm (b) after irradiation by a 5-GW cm^{-2} pulse from the CCL. The scale is 11.8 μm div^{-1}.

Thus, only a small fraction (estimated as 10 %) of the CCL output energy incident on samples was spent to excite ytterbium. A grater part (up to 70 %) of the CCL energy was transformed to stimulated scattering due to nonlinear interaction with the medium and was spent to form intense acoustic waves accompanied by heat release in the medium. The thermal energy required for heating and melting of the above-mentioned Yb : YAG crystal cylinder was estimated as 30 mJ. At the same time, the thermal energy remaining in the medium during the formation of inversion and generation and due to stimulated scattering did not exceed, according to estimates, 10 mJ, i.e. it was insufficient for melting of the material. This suggests that structural variations in the surface layer of samples (Fig. 7) can be produced by intense acoustic waves appearing during the SBS of pump radiation.

Thus, the ytterbium-doped medium during the SBS of pump radiation proved to be divided into a layer of thickness $l \approx 100$ μm with the high inversion and the main part of the sample to which pump radiation hardly penetrated.

4. Stimulated emission in the ytterbium-doped active medium upon stimulated scattering of pump radiation

Figures 2–5 demonstrate the integrated (per pulse) temporal pictures and broadband and narrowband lasing spectra of ytterbium. These two types of emission correspond to different laser pulses appearing at different stages of the development of lasing. We can distinguish two such stages: the first one is the development of lasing during irradiation of a sample by the pump pulse, and the second one is lasing after the end of the pump pulse. We attribute broadband lasing in the crystal and glass to laser pulses appearing at the first stage.

Consider the conditions of inversion formation and lasing development at the first stage by using a model assuming the appearance of shock acoustic waves in the medium during the SBS of pump radiation. Excitation of ytterbium ions to the $^2F_{5/2}$ metastable level and formation of a grating of longitudinal acoustic waves (Fig. 8) occur simultaneously in a thin layer of the medium. The grating period Λ is related to the pump wavelength λ_p and the refractive index of the medium n_p by the expression $\Lambda = \lambda_p/(2n_p)$ [14]. By assuming for the estimate that $\lambda_p \approx 0.92$ μm, we obtain $\Lambda \lesssim 0.3$ μm. The period of the acoustic wave is $T = \lambda_p/(2n_p V)$, where V is the sound speed. For the glass, we have $T \approx 70$ ps, and for the YAG crystal, $T \sim 50$ ps.

Intense acoustic waves propagating in the medium can strongly affect the spatial distribution of inversion. Indeed, conditions are produced for excitation of high-frequency vibrations of the medium and SRS on the fronts of shock waves. The scattering parameters [12] show that a broad phonon spectrum is excited upon SRS, including phonons with energies ~ 1000 cm^{-1} near the high-frequency boundary of the phonon spectrum in glasses and crystals [19, 20]. The energy of such phonons is sufficient for the population of the Stark components of the $^2F_{7/2}$ level lying above the ground level of ytterbium (Fig. 9). The redistribution of the population of Stark levels occurs during several picoseconds [1]. Due to the phonon population on the fronts of shock waves, the inversion for transitions from the $^2F_{5/2}$ level to the Stark components of the $^2F_{7/2}$ level lying above the ground level is decreased, preventing the development of lasing. At the same time, due to the rapid decrease of pressure and dynamic cooling of the medium, which occurs behind the fronts of shock waves (Fig. 8), the population of the Stark components of the $^2F_{7/2}$ level is rapidly depleted, resulting in the inversion jump. As a result, a distribution (with period Λ) of thin (less than 0.3 μm) layers with the high inversion is established in the medium for a short time ($t_{inv} < T$). During the propagation of an acoustic wave, the inversion regions are displaced. After the time T, the same inversion distribution over layers again reestablished. Thus, upon the SBS and SRS of pump radiation, amplification can appear at transitions between the $^2F_{5/2}$ level and Stark components of the lower $^2F_{7/2}$ level, including transitions in the short-wavelength region ($\lambda < 1.03$ μm), which are not observed usually in experiments with ytterbium lasers.

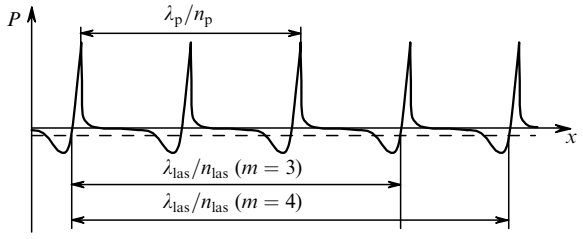

Figure 8. Illustration of the conditions for producing inversion and stimulated emission in the region of propagation of a periodic sequence of shock acoustic waves in the active medium. The dependence of the pressure profile P in the acoustic wave on the coordinate x along the pump beam is shown. The dashed straight line indicates the pressure at which inversion is produced. The possible relations between the pump wavelength λ_p and laser wavelength λ_{las} satisfying condition (1) are given.

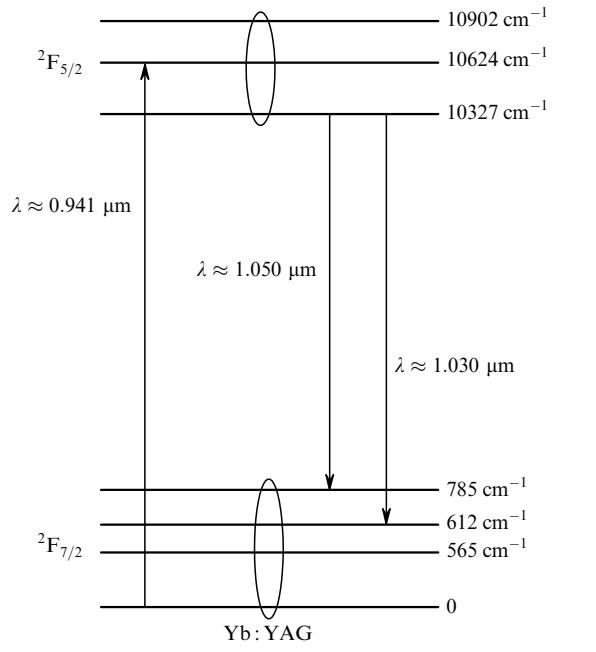

Figure 9. Energy level diagram of Yb^{3+} ions in a Yb : YAG crystal [1]. Ovals combine the Stark components of levels with rapid ($\sim 10^{-12}$ s) thermal relaxation.

The formation of inversion in the region of propagation of acoustic waves produces the conditions for generation of short radiation pulses in the medium. Indeed, a distributed feedback (DFB) laser [21] appeared in fact in our experiments in the acoustic grating region. Such a laser operates without an external resonator and can emit picosecond pulses [21–23]. Unlike dye DFB lasers based on a photo-induced sinusoidal grating in the medium [21–23], the high-contrast DFB structure was formed under our conditions due to modulation of the medium parameters (refractive index, inversion) during the propagation of a sequence of intense acoustic waves.

The possibility of creating a DFB laser on a hypersonic acoustic grating was discussed already in pioneering paper [21]. The length of the DFB structure in the SBS region is ~ 100 μm; in this case, the travel time t' of a photon in the structure is much shorter than the round-trip transit time τ in the ytterbium laser resonator ($\tau = 2L/c \approx 100$ ps). The possibility of lasing in the acoustic wave region without the resonator is confirmed by experiments. Lasing during the pump pulse was observed both in samples mounted inside the resonator and in samples without the resonator, in particular, in samples mounted at an angle to the pump beam axis. The generation of picosecond pulses in dye DFB lasers on a stationary grating pumped by nanosecond pulses occurs due to self-Q-switching ('blowing away' of the gain grating by the structure emission itself) [22, 23]. Unlike this, upon the SBS of pump radiation, a DFB structure moving in the medium appears with period Λ which can depend on the pump intensity (pressure in the medium). Under these conditions, the self-Q-switching in the DFB structure can be determined, apart from the mechanism considered above, by the rapid movement of the grating in the medium and by variations in its parameters. Picosecond pulses of duration $t < t_{\mathrm{inv}}$ could be generated in our experiments successively in these periodic inversion layers during their movement. The change in Λ should lead to scanning of the lasing spectral band over the gain profile in the medium. The temporal picture of ytterbium lasing at the first stage of its development was not investigated due to the lack of recording equipment with a proper time resolution. The shape and duration of laser pulses (the first laser pulses in oscillograms in Figs 2, 3, 5) were determined by the time resolution of the oscilloscope (~ 4 ns).

By considering the conditions for appearing stimulated radiation in the moving layer structure, we can interpret the features of broadband lasing spectra of the glass and Yb:YAG crystal (Figs 2–5). The emission of ytterbium appears at wavelengths $\lambda_{\mathrm{las}} > \lambda_{\mathrm{p}}$. This emission is amplified along the normal to the layer structure when the path difference between the layers involved in lasing is equal to the quantity multiple of λ_{las}. This synchronism condition between acoustic waves and lasing can be written in the form

$$\frac{\lambda_{\mathrm{las}} k}{n_{\mathrm{las}}} = \frac{\lambda_{\mathrm{p}} m}{2 n_{\mathrm{p}}}. \qquad (1)$$

Here, n_{las} is the refractive index of the medium for λ_{las}; and k and m are integers. It is important that the refractive index depends on pressure P in the medium: $n_{\mathrm{las}}, n_{\mathrm{p}} \sim P$. Pressure depends on the intensity of acoustic waves and the heat release in the medium upon pumping. The maxima of the spatial structure of the laser radiation field are located in regions with a decreased density, behind the fronts of shock waves (Fig. 8). Here n_{las} can take values lower than the refractive index n'_0 at the normal pressure. At the same time, the refractive index n_{p} on the fronts of shock waves can be larger than at the normal pressure. Under these conditions for $n_{\mathrm{las}} < n_{\mathrm{p}}$, relation (1) is fulfilled for $k = 1$ for small values of m ($m > 2$, $m = 3$, 4, etc., see, Fig. 8).

It follows from the relation $\Lambda = \lambda_{\mathrm{p}}/(2n_{\mathrm{p}})$ that, as the intensity of acoustic waves and heat release increase (with increasing P and n_{p}) for fixed λ_{p}, the period Λ of the grating decreases. This in turn leads to the blue shift of λ_{las}. Correspondingly, as P is decreased, the wavelength λ_{las} should shift to the red. Experiments confirm these conclusions. The shift of broadband lasing spectra with changing the pump intensity is illustrated in Fig. 3. One can see that the lasing spectrum of Yb:YAG shifts to the blue by 10 nm with increasing the CCL pulse energy from 100 to 150 mJ. Note that the shift of the emission region of DFB lasers with changing pressure in the medium was observed in dye lasers [22].

The inhomogeneous distribution of the pump intensity with the maximum at the beam axis gave rise to the transverse gradient of pressure $P(r)$ in the region of propagation of acoustic waves. Because of this gradient, for regions with different pump intensities (at the beam axis and its periphery) relation (1) is fulfilled for different values of m. These values can correspond to the regions of the broadband spectrum shifted in the wavelength scale and over the slit height (see Figs 2–5). In the axial region with the maximum pressure ($r \approx 0$, the lower part of spectrograms), lasing is developed in the short-wavelength part of the spectrum. The lasing spectra in the regions with the lower pump intensity ($r > 0$) are shifted to the red (Figs 2–5). Note that lasing in the DFB structure with a period multiple of the lasing wavelength ($m = 2$, 3) was observed in a dye laser [24].

The regions of the broadband spectrum should be located on the wavelength scale in accordance with possible radiative transitions in the ytterbium glass and Yb:YAG crystal. According to the energy level diagram presented in Fig. 9, the emission of Yb:YAG in the spectral region under study (Figs 2 and 3) can be determined by transitions between the two lower components of the metastable $^2F_{5/2}$ level with energies 10327 and 10624 cm^{-1} and three components of the $^2F_{7/2}$ level with energies 565, 612, and 785 cm^{-1}. A comparison of the emission spectra of the ytterbium glass (Figs 4, 5) with the luminescence spectrum of a similar ytterbium-doped phosphate glass [25] shows that lasing in a broad spectral region also should be related to several transitions between the $^2F_{5/2}$ and $^2F_{7/2}$ levels in the glass. In each spectral region, lasing in the DFB structure develops in the active medium within the part of the gain line corresponding to the radiative transition in ytterbium which is resonant for the given period of acoustic waves. Thus, a large width of lasing spectra of ytterbium-activated materials (Figs 2–5) can be caused not only by the generation of short pulses in the DFB structure upon emission of thin layers of the active medium but, as explained above, by the shifts of λ_{las} with changing the pump intensity.

Relation (1) can be used to estimate pressure on the fronts of shock acoustic waves. By assuming that lasing appears on the trailing edges of shock waves when $n_{\mathrm{las}} = n'_0$ (n'_0 is the refractive index for the unperturbed medium) or even when $n_{\mathrm{las}} < n'_0$ (the maxima of the lasing wave are

located in regions with the reduced density), we can calculate the corresponding values of n_p for $m = 3, 4, 5$ from (1). The dependences $n_p(n_{las})$ for glass calculated for the three values of the parameter m are presented in Fig. 10a. The dependence of the refractive index on the static pressure is known for a number of media [26–28]. According to [28], the coefficient dn/dP for glass is $\sim 0.13 \times 10^{-5}$ bar^{-1}. By using this value for estimates, we obtain from dependences $P(n_{las})$ (Fig. 10b) that pressure on the fronts of shock waves can achieve 100 GPa.

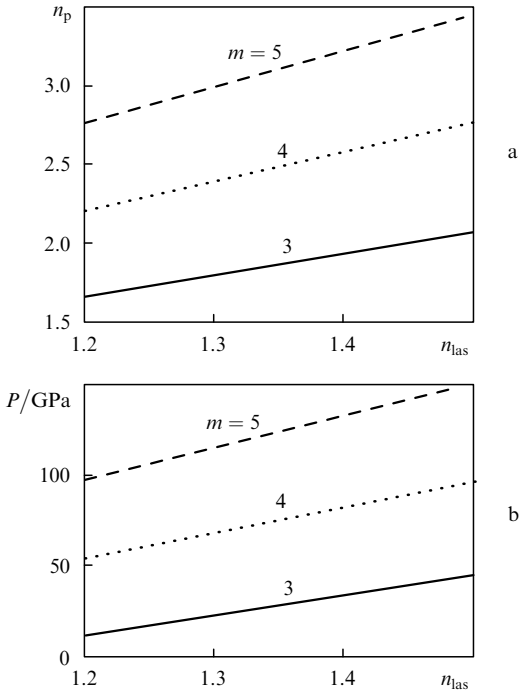

Figure 10. Dependences of the refractive index n_p of glass for pump radiation (a) and pressure P at the shock wave front (b) on the refractive index n_{las} behind the shock wave front for different m and $\lambda_p \approx 0.92$ μm, $\lambda_{las} = 1.00 - 1.03$ μm.

Unlike the studies of dye DFB lasers with the sinusoidal grating, where high-directional lasing was not observed [22], in our experiments a contrast grating (a structure consisting of thin inversion layers of thickness much smaller than λ_{las}) appeared upon SBS of pump radiation. The formation of the sharp angular radiation pattern of broadband lasing of the Yb : YAG crystal and ytterbium glass (Figs 2–5) should be discussed separately. To explain the possibility of the appearance of radiation beams with the angular divergence smaller than the diffraction limit corresponding to the lasing region size, it is necessary to discard the generally adopted concept of the propagation of photons in the form of a travelling wave. It should be assumed instead that individual photons propagating at the speed of light form the field maxima (minima) and nodes spatially fixed along their propagation direction [13]. In this case, for example, the equation for the electric component E_i of the field of the ith photon with the wavelength λ propagating along the x axis has the form $E_i = E_{i0} \sin(kx - \varphi_{i0})$, where $k = 2\pi/\lambda$ is the wave vector; E_{i0} and φ_{i0} are the field and phase at the point with coordinate x_0, and $x = x_0 + ct$. Note that this assumption about the properties of a photon does not contradict, generally speaking, the well-known properties of electromagnetic waves, which were verified many times experimentally and theoretically. For example, a plane monochromatic linearly polarised travelling wave emerging through a semitransparent mirror from the resonator of a single-frequency cw laser with the long active medium (longer than λ) can be 'constructed' from photons having the same frequency but located at different sites (and having different phases) in the resonator. In the case of the homogeneous distribution of emitting centres in the active medium of such a laser, the total photon field is formed on the output mirror (after many round-trip transits of radiation in the resonator) whose phase changes as $\varphi \sim \omega t$ ($\omega = 2\pi c/\lambda$). The propagation of each of these photons outside the resonator described by the law $E_i = E_{i0} \sin(kx - \varphi_{i0})$ produces the total effect of a travelling wave of the form $E = E_0 \sin(kx - \omega t - \varphi_0)$ propagating along the x axis (similarly to the effect of 'running fire' propagating by lamps in a Christmas tree garland).

Unlike a usual laser with the extended active medium in the resonator, in our experiments radiation was formed in a structure consisting of thin inversion layers. The regions with reduced pressure behind the front of shock waves, shown in Fig. 8, represent as if the 'instant photograph' of the spatial arrangement of such a structure. The photons with the wavelength resonant with the structure, $\lambda_{las}/n_{las} = m\Lambda$, will occupy different spatial positions in the 'photograph' with respect to the layers of thickness $l_{inv} \ll \lambda_{las}/n_{las}$. And only a small part of the total number of photons in the 'resonator' of our DFB laser will coincide in position and phase with the inversion maxima in the medium and, therefore, will be amplified efficiently during the lifetime $t_{inv} < T$ of the layers of the given spatial configuration, forming a beam.

The diffraction divergence of any radiation beam is caused by the interference of photons with different phases contained in the aperture of this beam. The phase dispersion of photons distributed in the interval Δx along the beam can be estimated as $\Delta\varphi = 2\pi\Delta x/\lambda$. When the beam is limited by an aperture of diameter d, the direction to the first minimum of the far-field intensity distribution (half the angle α of the diffraction divergence of radiation) can be written in the form $\alpha \sim \lambda\Delta\varphi/(2\pi d)$. In the case of a travelling plane monochromatic wave, the phase dispersion $\Delta\varphi$ in the beam can achieve $\pm\pi$, as explained above. This gives the known estimate $\alpha \sim \lambda/d$ of the diffraction divergence angle for a beam limited by an aperture of diameter d. If the phase dispersion of photons is decreased, the diffraction divergence angle α decreases proportionally to $\Delta\varphi$. The group of such phased photons will form a beam with the sharp angular radiation pattern, which was observed in our experiments. 'The instant photograph' of the filed distribution in such a beam can represent the contrast periodic structure of antinodes and nodes and can noticeably differ from 'the instant photograph' of a travelling sinusoidal wave. During the movement of the structure containing inversion layers (after the acoustic wave), new groups of phased photons will be formed, and their frequency will shift with changing the structure parameters.

The model considered above explains the appearance of the sharp angular radiation pattern of the broadband lasing of ytterbium in the crystal and glass. In the case of a 'thick' sinusoidal grating, photons occupying different positions in space (which is equivalent to the large phase dispersion within the photon group) are amplified. This leads to the

increase in the radiation divergence. Thus, when a periodic spatial grating of thin inversion layers is produced in the active medium, the high-directional stimulated radiation of an ensemble of excited atoms can be observed in the optical range.

The propagation of laser radiation in thin soap films without the characteristic diffraction divergence was observed in [29]. We can assume that the two-dimensional periodic structure of molecules on the film surface has selecting properties with respect to photons, similarly to periodic thin inversion layers in our experiment. Due to the possibility of combining the spatial structure of the laser radiation field incident on the film with the particular microstructure of emitters (molecules) of the given site of the thin film, the groups of phased photons are selected, which propagate in the soap film along curvilinear paths ('whiskers') and escape from it in the form of collimated radiation beams [29–31].

5. Features of the temporal picture and lasing spectra during the relaxation of the SBS excitation region in the ytterbium-doped active medium

Consider the conditions for the development of lasing in a resonator during the relaxation of the SBS excitation region in the active medium (second stage). Lasing develops in the resonator in the presence of the region of optical inhomogeneity in the active element – a thin layer of the medium with the inhomogeneous inversion distribution and gradient of the refractive index produced by pressure, temperature, and density gradients. Variations in the optical parameters of this layer and in the inversion level during relaxation of the SBS excitation region in the medium affect lasing parameters.

It follows from experiments that lasing in the resonator was predominantly developed at the periphery of the excited region in the active medium: the line spectra in Figs 2–5 are shifted with respect to broadband spectra upward along the slit height. Lasing in the resonator can develop already on the trailing edge of the pump pulse (Fig. 3). The line spectrum of the glass in Fig. 4 'grows' from the regions of the broadband spectrum, i.e. lasing in the resonator can 'pick up' broadband radiation. The 'seed' spectrum propagating in the resonator narrows down to the width of individual modes.

The generation of a train of nanosecond pulses in the resonator after the end of the pump pulse (see Figs 2, 3, 5) also confirms the existence of a small region in the medium with high inversion and high temperature caused by the SBS of pump radiation. The formation of a train of pulses can be explained by the dynamic unloading of the high-pressure region and rapid cooling of a thin active-medium layer. The decay of longitudinal acoustic waves carry energy away from the layer along the propagation direction of pump radiation. The inversion in the medium is recovered up to the threshold value for the generation of the next pulse due to the decrease in the population of the Stark components of the lower $^2F_{7/2}$ level caused by the pressure drop and rapid cooling of a thin layer. According to estimates, the 'escape' time of phonons at the sound speed from a layer with $l \leqslant 100$ μm is 100–200 ns. These estimates are in qualitative agreement with the time scales during the generation of a train of nanosecond pulses. The shift of the narrowband lasing region of the Yb:YAG crystal with changing the pump intensity, which was discussed in detail in [3], is explained by changes in the levels of inversion and losses in the active medium at transitions at 1.03 and 1.05 μm.

Figures 2, 5, 11 illustrate a number of features of narrowband lasing spectra. Figure 2 demonstrate the bending of a spectral line with respect to the vertical position of the spectrograph slit, which is observed in the 1.03-μm region. Such bent (or tilted) spectral lines were also recorded in other spectrograms [13]. The bending of the line in Fig. 2 means the wavelength of lasing at the same longitudinal mode (the number of nodes is preserved) changes from the centre to periphery of the excited region of the active medium. This corresponds to the development of lasing in some sites of the medium with a high pressure (refractive index) gradient from the beam centre to its periphery. It can be easily shown that λ_{las} shifts to the blue if the refractive-index gradient decreases from the beam axis to its periphery (Fig. 2). The pressure drop ΔP in the medium can be estimated from the spectral line shift. The frequency ω_q of the longitudinal mode of the resonator with the number of wavelengths λ_q over the resonator length $2L$ equal to q is described by the expression

$$\omega_q = \frac{\pi c q}{(L-\Delta l)n_0 + \Delta l n(r)}, \tag{2}$$

where Δl is the longitudinal size of the optical inhomogeneity region of radius r; n_0 is the averaged refractive index outside the nonlinearity region; and $n(r)$ is the refractive index in the nonlinear region. It follows from (2) that the change in the mode frequency ω_q during the displacement along the radius from r_1 to r_2 is

$$\Delta\omega_q = \frac{\pi c q \Delta l[n(r_1) - n(r_2)]}{[(L-\Delta l)n_0 + \Delta l n(r_1)][(L-\Delta l)n_0 + \Delta l n(r_2)]}. \tag{3}$$

By substituting the expression for q into (3) and assuming that $\Delta l n(r) \ll L n_0$, we obtain the dependence $\Delta n(r)$ of the change in the refractive index along the lasing region radius

$$\Delta n \simeq \frac{\Delta\lambda_q(r) L n_0}{\lambda_q \Delta l}. \tag{4}$$

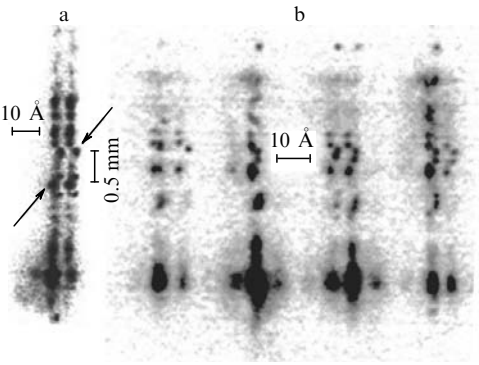

Figure 11. Fragments of lasing spectra of the Yb:YAG crystal at ~ 1.03 μm (a) and ytterbium glass in the region from 1.04 to 1.05 μm (b). The arrows in Fig. 11a indicate spectral regions with the shifted laser wavelength.

Here, $\Delta\lambda_q(r)$ is the wavelength shift along the radius. For $\Delta\lambda_q(r) \approx 1.4 \times 10^{-7}$ cm, $\lambda_q \approx 10^{-4}$ cm, $L \approx 2$ cm, $n_0 \approx 1$, and $\Delta l \approx 10^{-2}$ cm, the change in the refractive index is $\Delta n \approx 0.28$. By assuming that the change in the refractive index is produced only by the change in pressure along the radius caused by the different intensities of shock waves and using the value of dn/dP for glass from [28], we obtain $\Delta P \approx 30$ GPa.

The line spectra of the glass and Yb : YAG in Figs 5 and 11 obtained at the later instants of the lasing development (delays up to 300 ns) exhibit line discontinuities and breaks, and individual spots. This can be interpreted in the following way. After the end of the pump pulse, the energy stored in a thin layer of the medium is transformed to the energy of diverging (predominantly in the radial direction) acoustic waves. The processes of compression and rarefaction in the medium on the fronts and drops of these waves give rise to the opposite gradients of the refractive index in a sample. Figure 11b demonstrates two–three breaks of spectral lines, which probably correspond to the positions of the front of the shock wave diverging from the region centre at the instants corresponding to the appearance of individual lasing spikes in the ytterbium laser resonator. The breaks of spectral lines and shifts of their wavelengths gave an opportunity to observe lasing spots of size up to 100 μm (Fig. 11), which probably correspond to individual small emitting regions in the active medium. The angular divergence of radiation from a source producing a spot of size 100 μm at a distance of 1 m should be $\sim 10^{-4}$ rad, which is two orders of magnitude lower than the diffraction limit for the entire lasing region of size $r \approx 100$ μm. The observation of small lasing spots in the far-field zone can be explained by using the new concept of the photon nature presented above. A small region with a high gain in the resonator is in fact an angular selector of radiation, which collects photons synchronised in phase and direction into a collimated beam. The high-directional propagation of radiation from small sources was observed in experiments with thin films [30, 31].

The shifts of the lasing wavelength observed over the slit height (Fig. 11) allow us to estimate from (4) pressure drops between different regions of the medium. The spectral shift by 3 Å (Fig. 11a) gives the pressure drop ΔP produced by an acoustic wave equal to ~ 5 GPa.

6. Conclusions

We have studied lasing in Yb : YAG crystal (20 % of Yb) and ytterbium glass (10 % of Yb) plates pumped by focused low-coherence 20–30-ns, 0.89–0.95-μm pulses from a F_2^+ : LiF colour centre laser. Under the SBS and SRS of pump radiation, nanosecond radiation pulses of ytterbium ions were observed in the spectral region from 1.00 to 1.06 μm. The spectral width of the pulses achieved 20 nm in Yb : YAG and 50 nm in the ytterbium glass. The broadband lasing of ytterbium was observed in the active medium region of diameter less than 200 μm. The angular directivity ($10^{-3} - 10^{-4}$ rad) of radiation from the lasing region was more than an order of magnitude higher than the diffraction limit.

The experimental data on lasing in the Yb : YAG crystal and ytterbium glass have been explained within the framework of the physical model assuming the generation of longitudinal shock acoustic waves in the region of excitation of SBS of pump radiation, which produce a periodic grating of thin inversion layers moving in the medium. Inversion between the $^2F_{5/2}$ and $^2F_{7/2}$ levels of ytterbium can periodically appear in different sites of the active medium for a short time due to rapid relaxation ($\sim 10^{-12}$ s) of the population of the Stark components of the levels during the propagation of a sequence of acoustic waves in the medium. The lifetime t_{inv} of the structure containing inversion layers of the given configuration can be estimated as $t_{inv} \approx 0.1T \leqslant 10$ ps (the period of the acoustic grating is $T < 100$ ps). The presence of the spatial structure of inversion layers allows us to treat the ytterbium-doped medium upon the SBS of pump radiation as a DFB laser. Because the photon transit time in the structure of length $l \leqslant 100$ μm is $t' < 0.3$ ps $< t_{inv}$, we can assume that the inversion medium emits superradiant picosecond pulses [32]. A change in the grating parameters with changing the pump intensity (pressure in the medium) leads to the scan of the laser wavelength within the gain band of the active medium. This explains a large width of the lasing spectra of ytterbium. A set of thin emitting layers phased by the acoustic wave produces a sharp angular laser radiation pattern.

Experiments on the SBS and SRS of CCL radiation and the type of damages produced in the crystal and glass in the region of SBS excitation also correspond to the model assuming the generation of shock acoustic wave in the medium. The data obtained in the study suggest that shock acoustic waves generated upon SBS of low-coherence radiation in the medium should be treated as a real physical object. The directional action of high-energy phonons produces structural changes near the surface of glass and crystal samples, which were observed in our study. The pressure level on the fronts of shock waves was estimate as tens of gigapascal. We also observed volume damages in glasses and crystals in the form of spherical cavities, which were probably caused by the radial collapse of shock acoustic waves generated upon the SBS of CCL radiation. The formation of shock acoustic waves during the self-focusing of a laser beam can explain the nature of the well-known filament damages of optical media [12].

Our study of the broadband lasing of ytterbium expands the spectral range of lasing of ytterbium-doped media. At the same time, it is necessary to study further the broadband radiation source itself, which represents a medium containing ordered inversion layers. The detailed physical picture of the formation of inversion and short high-directional radiation pulses in thin layers in a medium is still to be determined. We used a CCL to produce inversion layers in the ytterbium-doped active medium. Similar emitting structures can be also formed in other laser materials by using one or several radiation sources to excite the medium and produce an acoustic grating. Media containing ordered emitting structures can be used as high-directional radiation sources in different spectral regions.

We interpreted the experimental data on the formation of a sharp angular radiation pattern ($10^{-3} - 10^{-4}$ rad) emitted from a region of size smaller than 100 μm by using the new concept of the spatial distribution of the electromagnetic field of photons not in the form of a travelling wave but with the field antinodes and nodes arranged in fixed positions along the radiation beam. This concept permits analysing the interaction of the electromagnetic radiation with matter in spatial regions comparable with the

radiation wavelength (or even smaller than the wavelength). Note also that the novel view on the photon nature can require the transformation of still existing views on a number of presently accepted fundamental physical concepts.

Acknowledgements. The authors thank T.T. Basiev, V.A. Konyushkin, B.I. Denker, and V.B. Semenov for placing laser materials at our disposal, A.A. Kaminsky for his interest in this work, and I.G. Zubarev, S.I. Mikhailov, A.I. Erokhin, and Yu.Yu. Stoilov for useful discussions.

References

1. Krupke W. *IEEE J. Sel. Top. Quantum Electron.*, **6** (6), 1287 (2000).
2. Dong J., Bass M., et al. *J. Opt. Soc. Am. B*, **20** (9), 1975 (2003).
3. Basiev T.T. et al. *Kvantovaya Elektron.*, **34**, 1138 (2004) [*Quantum Electron.*, **34**, 1138 (2004)].
4. Tokita S., Kawanaka J., Fujita M., et al. *Appl. Phys. B*, **80**, 635 (2005).
5. Dong J., Shirakawa A., Ueda K., et al. *Opt. Lett.*, **32** (13), 1890 (2007).
6. Bisson J.-F., Fredrich S., Kouznetsov D., et al. *Appl. Phys. Lett.*, **90**, 201901 (2007).
7. Bourdet G., Chanteloup J.-C., Fulop A., et al. *Proc. SPIE Int. Soc. Opt. Eng.*, **5478**, 4 (2004).
8. Nakai S., Hiuma T., Izawa Y., et al. *Book of Abstracts of the 29-th ECLIM* (Madrid, 2006) p. 59.
9. Pati B., Wall K., in *Advanced Solid-State Photonics 2007. Technical Digest* (Washington: OSA, 2007) report MC2.
10. Bayramian A. et al., in *Advanced Solid-State Photonics on CD-ROM. Technical Digest* (Washington: OSA, 2008) report MC1.
11. Fredrich-Thornton S., Huber G., et al., in *Advanced Solid-State Photonics on CD-ROM. Technical Digest* (Washington: OSA, 2008) report WB13.
12. Bykovsky N.E. http://ellphi.lebedev.ru/12/pdf16/pdf.
13. Bykovsky N.E. http://ellphi.lebedev.ru/17/pdf36/pdf.
14. Starunov V.S., Fabelinskii I.L. *Usp. Fiz. Nauk*, **98**, 441 (1969).
15. Ritus A.I. *Trudy FIAN*, **137**, 3 (1982).
16. Ready J.F. *Effects of High Power Laser Radiation* (New York: Academic Press, 1971; Moscow: Mir, 1974).
17. Polyakova A.L. *Pis'ma Zh. Eksp. Teor. Fiz.*, **4**, 132 (1966).
18. Polyakova A.L. *Pis'ma Zh. Eksp. Teor. Fiz.*, **7**, 76 (1968).
19. Gorelik V.S. *Kvantovaya Elektron.*, **37**, 409 (2007) [*Quantum Electron.*, **37**, 409 (2007)].
20. Banishev A.F. *Cand. Diss.* (Moscow, Moscow Institute of Physics and Technology, 1983).
21. Kogelnik H., Shank C.V. *Appl. Phys. Lett.*, **18** (4), 152 (1971).
22. Bor Z., Muller A. *IEEE J. Quantum Electron.*, **22** (8), 1524 (1986).
23. Katarkevich V.M., Rubinov A.N., et al. *Kvantovaya Elektron.*, **23**, 1091 (1996) [*Quantum Electron.*, **26**, 1061 (1996)].
24. Bjorkholm J., Shank C. *Appl. Phys. Lett.*, **20** (8), 306 (1972).
25. Koch R., Clarkson W., et al. *Opt. Commun.*, **134**, 175 (1997).
26. Zha C.S., Hemley R.J., et al. *Phys. Rev. B*, **50** (18), 13105 (1994).
27. Weinstein B.A., Zallen R., et al. *Phys. Rev. B*, **25** (2), 781 (1982).
28. Alcock R., Emmony D. *J. Appl. Phys.*, **92** (3), 1630 (2002).
29. Stoilov Yu.Yu. *Usp. Fiz. Nauk*, **174**, 1359 (2004).
30. Startsev A.V., Stoilov Yu.Yu. Preprint FIAN, No. 6 (Moscow, 2007).
31. Startsev A.V., Stoilov Yu.Yu. Preprint FIAN, No. 5 (Moscow, 2008).
32. Andreev A.V. *Usp. Fiz. Nauk*, **160**, 1 (1990).